International Journal of Fatigue 55 (2013) 245–256

Contents lists available at SciVerse ScienceDirect

International Journal of Fatigue

journal homepage: www.elsevier.com/locate/ijfatigue

# Effect of quality control parameter variations on the fatigue performance of ultrasonic impact treated welds

Rana Tehrani Yekta, Kasra Ghahremani, Scott Walbridge *

*Department of Civil and Environmental Engineering, University of Waterloo, Canada*

ARTICLE INFO

*Article history:*
Received 25 April 2013
Received in revised form 11 June 2013
Accepted 21 June 2013
Available online 9 July 2013

*Keywords:*
Ultrasonic impact treatment (UIT)
Quality control
Structural steel welds
Compressive under-loads
Fracture mechanics

ABSTRACT

Fatigue tests were conducted of steel non-load carrying filet welded attachments subjected to ultrasonic impact treatment (UIT) at various levels simulating proper, under-, and over-treatment. Two loading histories were investigated: one constant amplitude and one with high compressive under-load cycles. Local properties were measured, finite element (FE) analyses were performed to obtain stress concentration factor (SCF) distributions for the measured weld toe geometries, and a fracture mechanics model was validated and used to investigate the effects of the local property variations on the fatigue life. UIT significantly improved the fatigue lives of the welded specimens in all cases. A strong correlation was seen between the measured indent depth and the local residual stresses and microhardness. The fracture mechanics analysis predicts the fatigue performance of the specimens and finds it to be most sensitive to variations in the residual stresses and initial defect depth.



## 1. Introduction

Residual stress-based post-weld treatments (PWTs) can be an effective means of improving the fatigue performance of welded structures. With these treatments, the objective is to introduce compressive residual stresses by plastically deforming the weld toe, in order to slow or stop the propagation of fatigue cracks. Needle and hammer peening are well studied and established examples of residual stress-based PWTs. Their effectiveness for increasing fatigue life has been demonstrated in numerous studies (e.g. [1–3]). Models have been developed for predicting their effect on fatigue performance (e.g. [2,3]). Methods for proper execution and quality control are described and the resulting fatigue life increase is recognized in several recommendations and codes (e.g. [4–6]).

Ultrasonic impact treatment (UIT) is a relatively new residual stress-based PWT, which has received considerable attention over the last decade. As discussed in [7], UIT was first developed in the former Soviet Union. UIT is similar to needle or hammer peening in many respects. An important difference is that rather than using a pneumatic tool, which causes needles or a single hammer-like rod to impact the weld surface at a frequency of 25–100 Hz, with UIT, the weld is impacted by a small number of rods vibrating at a higher frequency on the order of 18,000–27,000 Hz. UIT offers a number of advantages over conventional peening. First and foremost, it is a much quieter device, which vibrates at a lower intensity, so that an operator can use it for longer periods of time before tiring.

Numerous experimental studies of UIT have been reported recently in the literature. Tests of fatigue details on large-scale girder specimens are reported in [7,8]. Based on the results of these tests, it is proposed that the detail category (according to [9]) for certain UIT treated details be increased by one level (i.e. Det. Cat. 'C' up to 'B' for transverse stiffener welds). Testing on UIT for application to high strength steel structures is summarized in: [10]. These studies have generally focused on constant amplitude, tension-only loading. Recent efforts to study the effectiveness of UIT under variable amplitude (VA) loading conditions are discussed in [11–13]. Efforts to study to the application of UIT applied under load, e.g. when retrofitting civil structures in-service, are discussed in [14].

The AASHTO Bridge Construction Specification [15] was recently updated with new clauses regarding the use of UIT on bridges, based on the research summarized in [7,8]. This standard recommends "as a guide, not a requirement" a final indent depth due to UIT falling within the range of 0.25–0.5 mm. An ideal notch radius of 3 mm is recommended. Additional guidelines concerning UIT application and qualitative quality control procedures are also provided in this reference.

Efforts are underway to consolidate the research conducted to date on UIT by various research groups. For design of welds treated by UIT (or "high frequency mechanical impact"), 228 data points (under constant amplitude, tension only loading) are used in [16] to develop strength improvement factors that account for the increased benefit of the treatment when applied to higher strength steels. A similar approach is used in [17] to evaluate various "local

* Corresponding author. Address: Department of Civil and Environmental Engineering, University of Waterloo, 200 University Avenue West, Waterloo, Ontario N2L 3G1, Canada. Tel.: +1 (519) 888 4567x38066; fax: +1 (519) 888 4349.
*E-mail address:* swalbrid@uwaterloo.ca (S. Walbridge).

0142-1123/$ - see front matter © 2013 Elsevier Ltd. All rights reserved.
http://dx.doi.org/10.1016/j.ijfatigue.2013.06.023

approaches" for predicting the fatigue life increase due to UIT, including the hot-spot stress and notch stress methods.

While the evidence appears to be mounting that UIT is an effective means of increasing fatigue life, when applied properly, a number of gaps in the state-of-knowledge remain unaddressed. Although guidelines now exist for the evaluation of treatment quality, it appears that they have been established primarily based on "best practice", and without any systematic investigation of the effects of under- or over-treatment on fatigue performance. Civil infrastructure owners who are specifying PWTs to retrofit existing structures have expressed a desire to know the consequences of deviations from the quality control guidelines, so that they can properly assess the risk of using this retrofitting approach. Among other things, they are particularly interested to know if over-treatment can result in irreparable damage or if improper treatment of any kind can reduce fatigue performance. These questions are particularly important in retrofit applications (in comparison with treatment of a new component during the shop fabrication), where the consequence of rejecting a treated weld can be extremely high.

Against this background, the current study was undertaken with the goals of: (1) examining the fatigue performance of structural steel welds subjected to UIT at various levels simulating proper, under-, and over-treatment, (2) relating the fatigue performance of the treated welds to geometric and metallurgical properties that can be measured to control the treatment quality, and (3) using the experimental results to validate a predictive model and make recommendations concerning the quality control of UIT for the retrofitting of welded civil structures, such as existing steel highway bridges.

For this study, fatigue tests were conducted of non-load carrying filet welded attachments subjected to proper, under-, and over-treatment. Local properties were measured, finite element (FE) analyses were performed to determine the effect of the measured weld toe geometry on the stress concentration factor (SCF) distribution, and a fracture mechanics model was validated and used to investigate the effects of the measured variations in the local properties on the predicted fatigue life. The main original aspects of this work are believed to be the fatigue testing of under- and over-treated welds, the use of a loading history containing compressive underloads, and the fracture mechanics analysis of UIT effects. In the following sections, the employed methods and key results are summarized. Additional details regarding the fatigue testing, local property measurements, and FE analysis can be found in [19].

## 2. Fatigue test description

The specimens were fabricated from 300 mm wide CSA G40.21 350 W steel plates with a thickness of $T = 9.5$ mm (3/8″). 350 W steel is a mild, weldable structural steel grade with a nominal yield and ultimate strength of 350 MPa and 450–650 MPa (for plates with $T < 65$ mm) and the following chemical composition: C (<0.23%), Mn (0.5–1.5%), P (<0.04%), S (<0.05%), Si (<0.4%), and other alloying elements or impurities (<0.1%) [18]. Transverse stiffeners were welded to the plates using the flux-cored arc welding (FCAW) process. The stiffened plates were then cut into 50 mm wide strips. The welds were inspected at this stage and the noted defects included minor lack of fusion at the weld root and a small offset of the stiffener plates on either side of the *T*-joint. No problems were observed, however, with the quality of the fatigue critical weld toes. Next, the specimens were treated by UIT using procedures and settings as shown in Table 1. Following the treatment, the specimens were "dog-boned" (see Fig. 1) using a computer numerical control (CNC) cutting machine [19].

In this study, treatment level was varied intentionally. Under-, over-, and properly treated specimens were tested. The under-treated specimens were tested to determine whether a fatigue life increase still occurs if the compressive residual stress level is reduced. The over-treated specimens were tested to determine whether over-treating can result in significant damage to the weld.

The treatments were performed either manually or using a robotic arm (of the kind used in automobile manufacturing). The arm was programmed to perform the treatment at various settings to simulate under-, over-, and proper treatment. Although UIT is normally performed manually when used to retrofit existing civil structures, it was thought that the use of the arm would lead to reduced variability and bias in parameters such as the treatment speed and duration. Proper treatment was assumed to correspond with a treatment speed of 10 mm/s and amplitude of 27–29 μm. Two kinds of under-treatment were considered: under-treatment by reducing the intensity (from 27–29 μm down to 18 μm) and under-treatment by increasing the treatment speed (from 10 to 20 mm/s). Over-treatment was simulated by reducing the treatment speed to 1 mm/s. This treatment speed was expected to represent an extreme lower bound for unintentional over-treatment. In all cases, the treatment was performed in four "passes" at angles (with respect to the larger plate) of 45°, 30°, 60°, and 45°.

Fig. 2 shows the treatment tool and a specimen after over-treatment using the robotic arm. In the case of over-treatment to this extent, significant flaking of the steel at the weld toe will be apparent afterwards, as can be seen in this figure. The presence of such flaking can be used as a means of quality control, if a weld inspector is present while the treatment is being performed.

Fig. 3 shows photos of weld toes that have been subjected to under-, over-, and proper treatment. The under-treated Group B UIT-induced groove has a visible line at the center along the location of the original weld toe. The under-treated Group C groove has individual impact marks visible and ridges between the passes. The over-treated Group D weld has significant evidence of flaking. The properly treated Group E and F welds are uniform, relatively smooth, and centered on the weld toe. More blending of the passes is apparent for the manually treated weld (Group F).

Two stress history types were investigated: constant amplitude (CA) loading and constant amplitude loading with periodic underload cycles (CA-UL). Compressive under-load cycles are known to be particularly severe for welds improved using residual stress-based PWTs such as UIT [3]. For each specimen, cycling was continued until failure or until a large number of cycles, *N* was reached without failure, in which case the test was considered a "run-out".

All fatigue tests were carried out under axial loading at testing frequencies below 23 Hz. For the CA loading, specimens were tested at stress ranges of 200, 225, and 250 MPa and a stress ratio ($S_{min}/S_{max}$) of $R = 0.1$. For the CA-UL loading, 1000 cycle blocks were repeated throughout the test. Of these, the first ten were underload cycles with stress ranges of 440, 500, or 556 MPa and a stress ratio of $R = -1$. The other 990 cycles had stress ranges of 200, 225, or 250 MPa respectively and a stress ratio of $R = 0.1$, similarly to the CA loading history. For plotting the data for the CA-UL tests, an equivalent stress range was calculated using Miner's sum and an S–N curve slope of $m = 3.0$.

The alternating Current Potential Drop (ACPD) technique was used during the fatigue tests to monitor the crack sizing and crack growth. The ACPD system used in this research consisted of a custom-made, magnetic two site ACPD array and TSC ACPD Mk IV instrument [3,20].

## 3. Fatigue test results

Table 2 shows the number of cycles to failure, *N*, for each tested specimen. The specimens that are underlined are "run-outs" and did not experience fatigue failures. Stress–life (S–N) results for

**Table 1**
Test matrix and specimen ID key.

| Group | Treatment | Method | Loading | $\Delta S$ (MPa)[a] | | |
|---|---|---|---|---|---|---|
| | | | | 200 | 225 | 250 |
| A | As-received (untreated) | – | CA | A1 | A2 | A3 |
| | | | CA-UL | A4 | A5 | A6 |
| B | Under-treated (reduced intensity) | Robotic | CA | B1 | B2 | B3 |
| | | | CA-UL | B4 | B5 | B6 |
| C | Under-treated (increased speed) | Robotic | CA | C1 | C2 | C3 |
| | | | CA-UL | C4 | C5 | C6 |
| D | Over-treated | Robotic | CA | D1 | D2 | D3 |
| | | | CA-UL | D4 | D5 | D6 |
| E | Properly treated | Robotic | CA | E1 | E2 | E3 |
| | | | CA-UL | E4 | E5 | E6 |
| F | Properly treated | Manual | CA | F1 | F2 | F3 |
| | | | CA-UL | F4 | F5 | F6 |

[a] Exact equivalent stress ranges for CA-UL tests = 206, 232, 258 MPa.

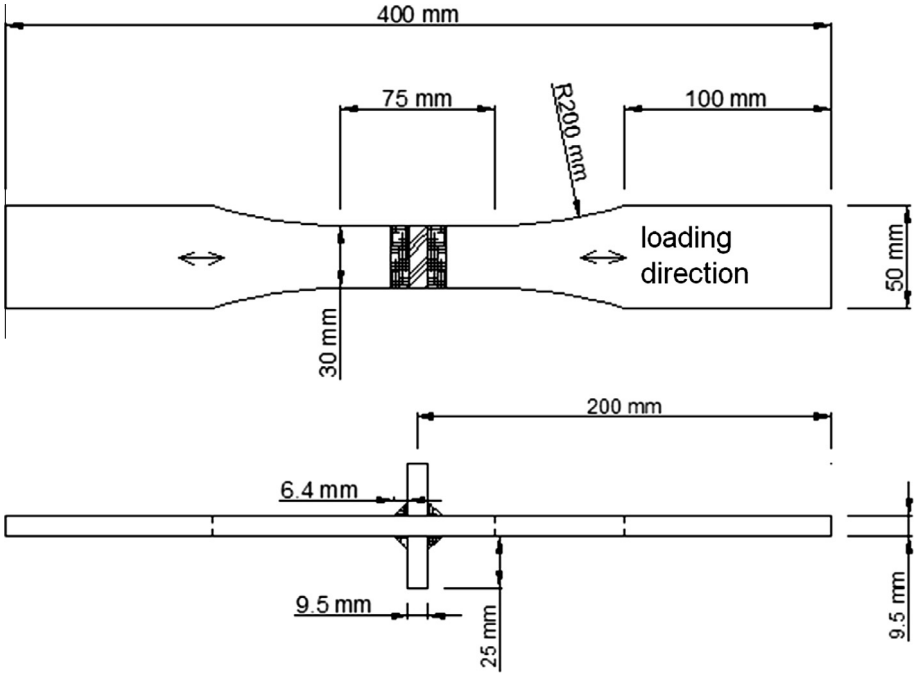


**Fig. 1.** Specimen geometry.

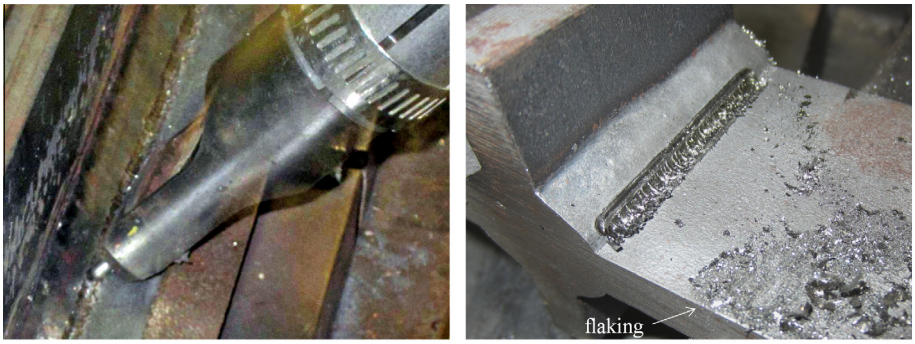


(a) UIT tool during manual treatment. (b) Weld toe after "over-treatment".

**Fig. 2.** Ultrasonic impact treatment.

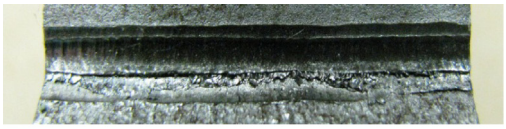

(a) Under-treated weld toe (Group B).

(b) Under-treated weld toe (Group C).

(c) Over-treated weld toe (Group D).

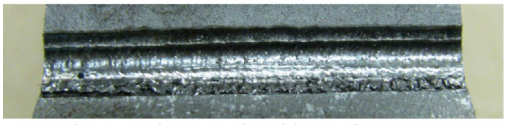

(d) Properly treated weld toe (Group E).

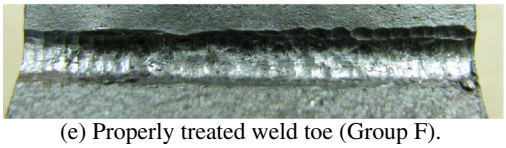

(e) Properly treated weld toe (Group F).

**Fig. 3.** Weld toes after proper, under-, and over-treatment.

the various specimen groups are plotted in Fig. 4. In this figure, the untreated specimens under CA and CA-UL loading are indicated with black and grey hollow symbols, respectively. The treated specimens under CA loading and CA-UL are shown with filled black and grey symbols.

Fig. 4(a) shows the S–N data for Groups A, E, and F (as-received and properly treated specimens). The AASHTO/CSA Detail Category 'C' design curve in this figure corresponds with a 97.7% survival probability [9,21]. It can be observed that all of the data points are above this curve. The fatigue lives of the as-received Group A specimens are closer to the Detail Category 'C' curve, whereas the fatigue lives of the Group E and F specimens (proper robotic and manual treatment) are shifted considerably to the right. The results from Group E and F fall more-or-less on top of each other, suggesting that there is little difference between these groups from the point of view of fatigue performance.

**Table 2**
Fatigue test results.

| Specimen | *N* | Specimen | *N* | Specimen | *N* |
|---|---|---|---|---|---|
| A1 | 248,383 | B1 | 2,099,320 | C1 | 1,537,837 |
| A2 | 166,821 | B2 | 3,510,188 | C2 | 8,210,202 |
| A3 | 105,487 | B3 | 1,773,851 | C3 | 3,031,499 |
| A4 | 202,874 | B4 | 3,667,264 | C4 | 3,564,413 |
| A5 | 185,887 | B5 | 4,159,128 | C5 | 4,796,216 |
| A6 | 94,746 | B6 | 816,298 | C6 | 460,835 |
| D1 | 3,436,785 | E1 | 3,021,835 | F1 | 7,692,074 |
| D2 | 1,932,685 | E2 | 2,244,137 | F2 | 4,207,209 |
| D3 | 450,647 | E3 | 2,753,812 | F3 | 1,175,500 |
| D4 | 2,649,012 | E4 | 8,873,089 | F4 | 3,141,363 |
| D5 | 876,309 | E5 | 2,064,805 | F5 | 1,938,919 |
| D6 | 485,965 | E6 | 533,901 | F6 | 561,878 |

*Note:* underline = run-out.

Fig. 4(b) shows the S–N data for Groups B, C, and D. For clarity, the data sets for Groups A and E/F have been replaced with curves corresponding with 50% and 95% survival probabilities. These curves were established using the methodology described in [22], which assumes that the data set follows a Gaussian log-normal distribution. The positions of these curves are then established using a regression model where log(*N*) is the dependent variable. According to [22], 10 or more data points should be used, if possible. Since the experimental program considered many variables and thus had only a few repetitions for each combination of variables, data sets were grouped together to increase the sample size, where possible. The statistical analysis for Group A therefore included the data points for CA and CA-UL loading, and the analysis for "properly treated welds" included all data points from Groups E and F. In the statistical analysis, the S–N curve slope, *m*, was allowed to vary and run-out points were not included. As discussed in [19], the use of a fixed *m* or inclusion of the run-outs had little effect on the general trends observed by comparing the survival probability curves.

In Fig. 4(b), it can be seen that a significant fatigue life increase results from the UIT application, even for the under- and over-treated specimens. Looking at this figure, it is difficult to assess visually whether the treatment level has a significant effect on the fatigue performance.

In order to investigate this question further, survival probability curves were established for two more data sets. The first was for all treated specimens in Groups B, C, D, E, and F. The curves for this data set were thought to represent survival probabilities of welds subjected to an unknown (or uncontrolled) treatment level. The second was for Groups B, C, and D, or in other words for the specimens that were intentionally under- or over-treated. These curves are plotted in Fig. 5(a) and defined in Table 3 where, *m* is the S–N curve slope and LOG(*M*) defines the vertical position, i.e.:

$$\mathrm{LOG}(M) = m \cdot \mathrm{LOG}(\Delta S) + \mathrm{LOG}(N) \quad (1)$$

In Fig. 5(a), it can be seen that the curve ranking for either the 50% or 95% survival probability is the same: the highest curve is for the properly treated specimens (Groups E and F), the lowest is for the intentionally under- or over-treated specimens (Groups B–D), and the curves for an unknown (or uncontrolled) treatment level fall in between. Notably, the spread between the curves for the treated specimens is small compared to the shift in the curve position due to treatment at any level. In [17], test results for welds subjected to UIT from a number of studies are analyzed and an S–N curve with a slope of $m = 5.0$ is recommended. In Table 3, it can be seen that the calculated S–N curves have this slope exactly when all of the test results for the treated welds from the current study are included. When only the properly treated welds are considered, the slope is somewhat flatter ($m = 6.41$).

Based on these observations, it can be concluded that quality control and treatment in accordance with the current "best practice"-based guidelines results in a higher fatigue performance. However, the treatment process is fairly robust in the sense that under- or over-treating within the investigated range of treatment parameter variations still results in a significant fatigue life increase.

Clearly, there would be value in conducting additional tests to increase the sample size for each combination of test parameters. In addition, some caution should be exercised in drawing definitive conclusions by comparing the curves for the treated welds in Fig. 5(a), since one parameter that could not be easily isolated was the effect of manual versus robotic treatment. The manual results are weighted more heavily in the statistical analysis of the properly treated welds (Groups E and F). It is possible that the results could therefore be biased, if the manual treatment was significantly more effective than the robotic treatment. There is a strong possibility that this is the case, since one of the suspected

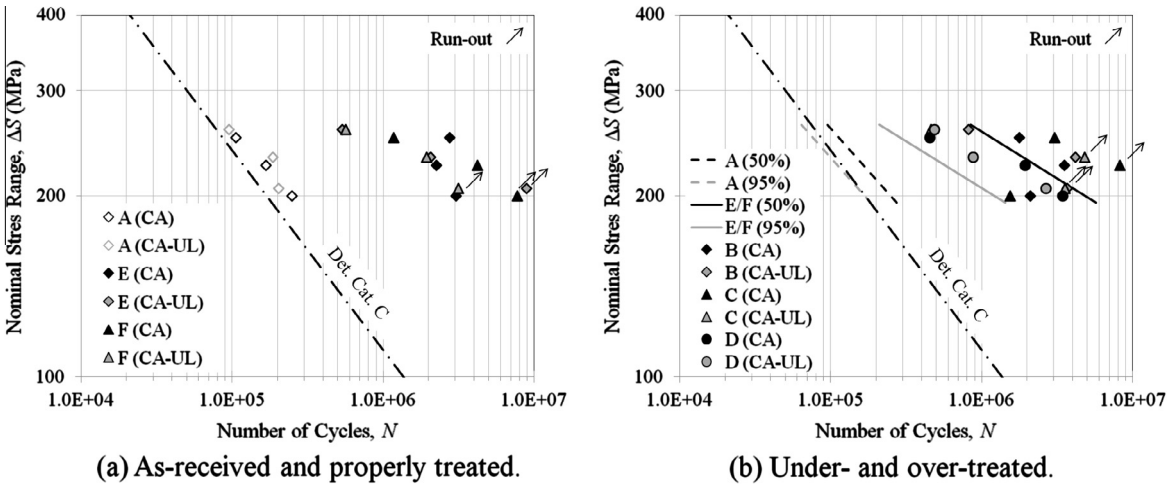


**Fig. 4.** Fatigue test results.

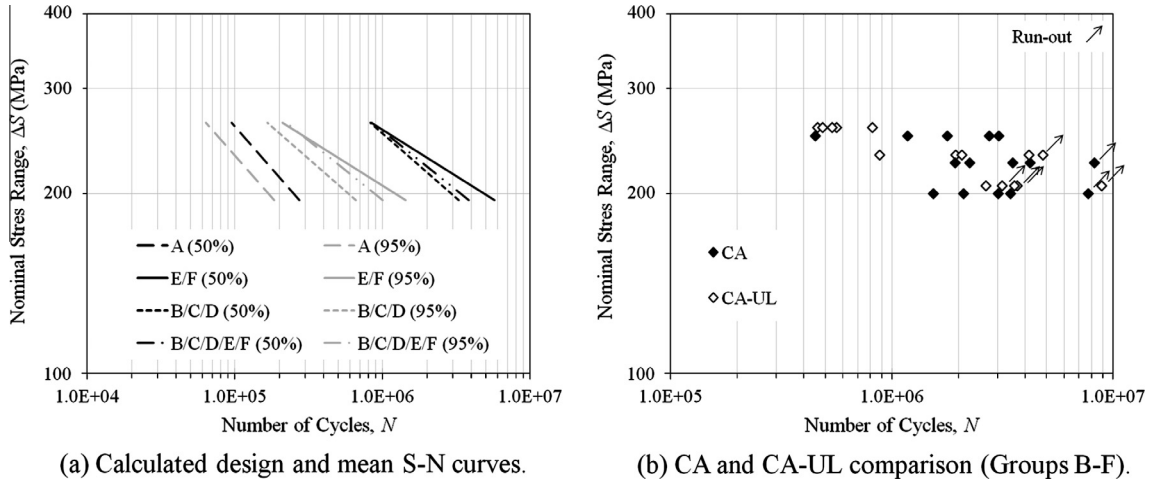


**Fig. 5.** Analysis of fatigue test results.

**Table 3**
Statistical analysis of test results.

| Group | $m$ | Mean (50%) | | Design (95%) | |
|---|---|---|---|---|---|
| | | LOG ($M$) | $\Delta S(2\times10^6)$ | LOG ($M$) | $\Delta S(2\times10^6)$ |
| A | 3.54 | 13.54 | 111.08 | 13.36 | 99.32 |
| B/C/D | 4.63 | 17.11 | 217.16 | 16.42 | 153.56 |
| B/C/D/E/F | 5.00 | 18.04 | 222.02 | 17.45 | 169.80 |
| E/F | 6.41 | 21.43 | 229.88 | 20.83 | 185.31 |

advantages of the manual treatment is that the human operator is better able to adjust to irregularities in the weld profile. It should be recalled, however, that the reason for using the robotic arm to treat the specimens was not to improve the level of treatment quality, but rather to reduce the bias when comparing the welds subjected to proper, over-, and under-treatment.

Based on a previous study on needle peened welds [3], the CA-UL loading history was thought to be a particularly severe one for residual stress-based post-weld treatments since, under certain circumstances, compressive under-loads can reduce crack closure and cause compressive residual stresses to relax due to nonlinear material effects. Fig. 5(b) shows a comparison of the S–N results for all of the treated specimens, which allows the results for the two investigated loading histories to be easily distinguished. Looking at this figure, it can be seen that the fatigue performance of the treated welds under CA-UL loading was systematically on the lower end at the highest stress range tested ($\Delta S \approx 250$ MPa). As the stress range decreases, however, this difference decreases, and at the lowest stress level ($\Delta S \approx 200$ MPa), there is no discernable difference between the results for CA and CA-UL loading. One possible explanation for this observed trend is that the scatter in the test results is expected to increase as the fatigue limit is approached, so it is possible that with the limited number of tests, the under-load effects are masked by the scatter in the test results at the lower stress ranges. Further testing would be needed, however, to confirm this hypothesis.

Fig. 6 shows example crack growth curves, obtained using the ACPD technique, for Specimens A6 (as-received) and F6 (proper, manual treatment). These are for the average of the two probe values at the critical weld toe. The probes were 10 mm apart and centered on the specimen [3]. As observed in [3], the effect of the treatment appears to be a crack growth rate reduction at the shallow depths (less than ~0.3 mm). At greater depths, the growth rates are similar for both specimens.

## 4. Local geometric and metallurgical properties

Weld toe geometry measurements such as the toe angle and radius before and after UIT application were obtained for each spec-

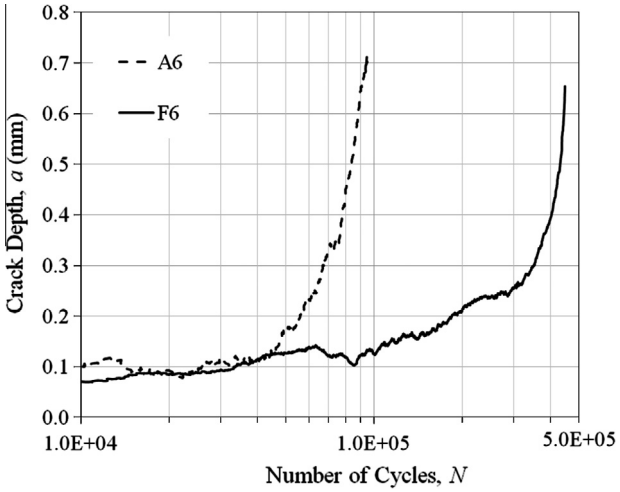


**Fig. 6.** Crack growth curves for Specimens A6 and F6.

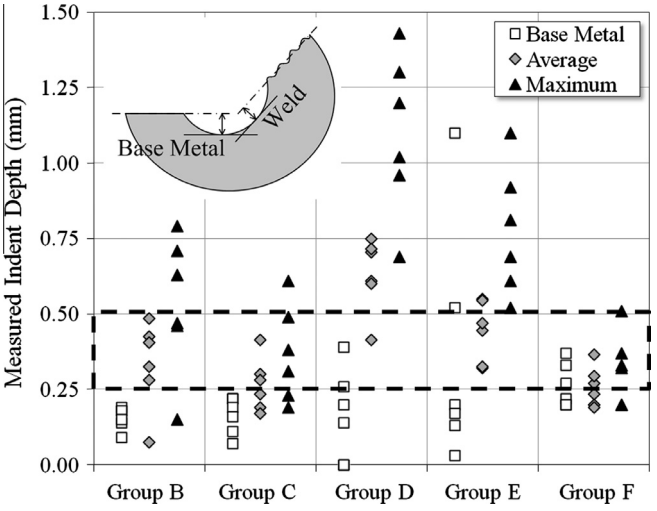


**Fig. 7.** Indent depth measurements.

imen. Sliced silicon weld toe impressions, taken before fatigue testing, were placed under a low power microscope, and photographed. Measurements of the geometric parameters were then made using AutoCAD. With the exception of the properly treated (Group E and F) weld toes, it was often difficult to define a single toe radius due to the irregular shape of the weld toe. The radius of the greatest indent depth on the base metal side was therefore recorded when multiple radii were present. The indent depth measurements were taken with respect to a best fit line along the base metal surface. This depth is similar to the one that weld inspectors measure to check for undercuts, when assessing weld quality. In addition, a best fit line was drawn along the surface of the weld, and a second indent depth was measured perpendicular to this line. The toe radius and indent depth measurements, obtained in this manner, are summarized in Table 4.

In Fig. 7, three ways of quantifying indent depth are compared: (1) indent depth from the base metal side only, (2) the average of the base metal and weld side indent depths, and (3) the maximum of these two depths. The rectangular region in Fig. 7 denotes the target indent depth range for recommended in [15]. It should be noted that in [15] only measurements of the base metal indent depth are discussed. In general, it was observed that for the robotic treatment, the tool was directed to a much higher degree towards the weld, rather than the base metal. Hence, the base metal indent depths were lower than expected for the robotically treated groups. However, the manually treated specimens in Group F all fall within or close to the target range. Using the average indent depth, based on measurements of a weld toe impression, it is easier to identify that the specimens in Group D are over-treated. On the other hand, while the average indent depths for the undertreated specimens fall below those for the specimens subjected to proper robotic treatment, the indent depths for the robotically undertreated specimens are similar to those for the specimens subjected to proper manual treatment. A similar trend is seen in the maximum indent depth results. Interestingly, the scatter in the various metrics is much smaller for the manually treated welds (Group F). This appears to support the hypothesis that it is easier to adjust for irregularities in the weld profile with manual treatment.

Vickers microhardness measurements were made in accordance with [23], using specimens cut and polished after fatigue testing. Eleven indentations were made along the expected crack path, starting at depth, $b = 0.1$ mm below the surface and then every 0.2 mm up to $b = 2.1$ mm. This process was repeated three times for each group. The resulting envelopes are presented in Fig. 8.

The measurements for the untreated group (Group A) were uniform with respect to depth below the surface and ranged from ~190 to 275 HVN. The first measurement at $b = 0.1$ mm is normally the highest in the treated specimens. Below this, the hardness decreases with depth. In general, it can be seen that the surface hardness is greatest for the over-treated group (D), followed by the properly treated groups (E and F). Under-treating by reducing the treatment intensity (Group B), has little effect on the surface hardness. On the other hand, under-treating by increasing the treatment speed (Group C) does result in a decrease in the surface hardness to a level similar to the untreated group (A).

Residual stress measurements were performed by Proto Manufacturing, a laboratory specializing in X-ray diffraction. The results are summarized in Fig. 9. Measurements were taken on specimens after testing, as well as on one untested specimen that had been manually treated with the other specimens in Group F, at depths of $b = 0.0$, 0.15, 0.3, 0.6, and 1.2 mm. In general, the near surface measurements were highly erratic [19] and did not follow any trends of similar measurements reported by others. One possible

**Table 4**
Weld toe geometry measurements.

| Group (mm) | Radius | | Indent depth (base metal side) | | | Indent depth (weld side) | | |
|---|---|---|---|---|---|---|---|---|
| | $\bar{x}$ (mm) | $s$ (mm) | $\bar{x}$ (mm) | $s$ (mm) | Max. (mm) | $\bar{x}$ (mm) | $s$ (mm) | Max. (mm) |
| B | 1.76 | 0.36 | 0.16 | 0.04 | 0.19 | 0.51 | 0.28 | 0.79 |
| C | 2.09 | 0.18 | 0.16 | 0.06 | 0.22 | 0.37 | 0.16 | 0.61 |
| D | 1.17 | 1.09 | 0.17 | 0.15 | 0.39 | 1.10 | 0.27 | 1.43 |
| E | 1.69 | 0.27 | 0.36 | 0.40 | 1.10 | 0.53 | 0.38 | 0.92 |
| F | 2.37 | 0.11 | 0.27 | 0.07 | 0.37 | 0.25 | 0.14 | 0.51 |

*Note:* $\bar{x}$ = mean, s = standard deviation.

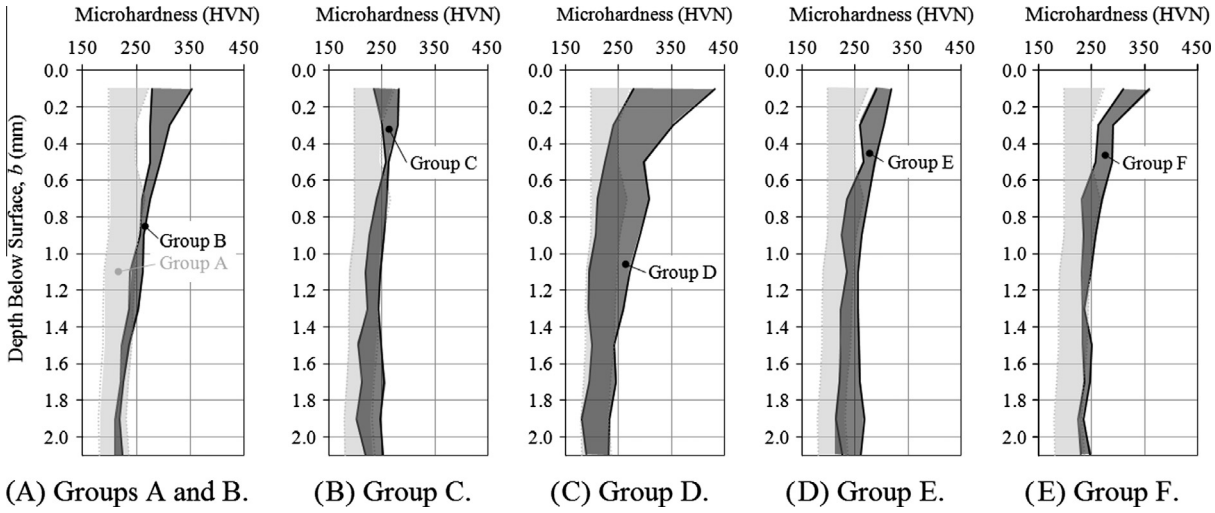


**Fig. 8.** Microhardness measurements.

explanation for this result is that the residual stresses relaxed or were otherwise altered by the high applied cyclic stresses (possibly exceeding the yield strength, $\sigma_y$) at the surface of the tested weld toes. Residual stress relaxation for welds subjected to UIT followed by cyclical loading has been observed by others, as discussed in [13,24]. For this reason, the $b = 0.0$ and 0.15 mm measurements in Fig. 9 are only plotted for the one specimen ($F^*$) that was subjected to X-ray diffraction measurements without prior loading. Looking at all of the measurements for depths, $b = 0.3$ to 1.2 mm in Fig. 9, it can be seen that the residual stresses in the untreated (Group A) weld were slightly compressive. It is believed that this was likely not the case for all of the untreated welds, based on previous measurements reported in [3] for the same weld procedure and specimen geometry. For the treated welds, the compressive residual stresses are highest in magnitude for the over-treated (Group D) specimens, followed by the properly treated (Groups E and F) specimens. The residual stress levels for the Group B and E specimens are similar. The residual stress magnitudes are much lower, however, for the Group C specimens, which were under-treated by increasing the treatment speed.

Several specimens of each type were sectioned, polished, and photographed with a low power microscope, in order to observe the effects of UIT on the grain structure and look for surface defects that could serve as initiation points for fatigue cracks. Fig. 10 shows example photographs taken from Specimens F2 and D2. In Fig. 10(a) and (c) it can be seen that the plastically deformed grains occur within 0.1–0.2 mm from the weld toe surface. In Fig. 10(b) and (d), fatigue cracks growing from surface defects can be seen. In the case of Specimen F2, a large crack is seen growing from a defect that is around 0.15 mm in depth. In the case of Specimen D2, the defect is a much larger fold running roughly parallel to the surface, with a depth approaching 1.0 mm.

## 5. Finite element analysis

The finite element (FE) method was used to predict geometric stress concentration factors (SCFs) along the crack path for the various treatment cases (disregarding residual stresses). In this context, the SCF is defined as the local elastic stress divided by the nominal, remotely applied stress, $S$. The nominal applied stress is taken as the applied load divided by the cross section area of the loaded plate. The ABAQUS CAE Version 6.11 software was used to perform the FE analysis. Sixteen specimens were chosen for mod-

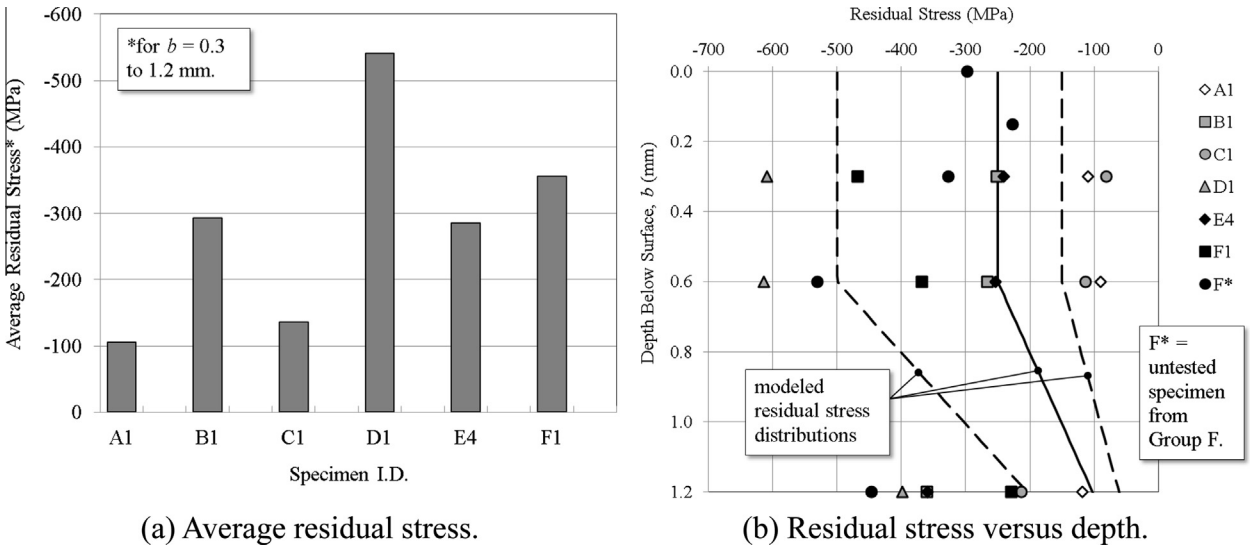


**Fig. 9.** Residual stress measurements.

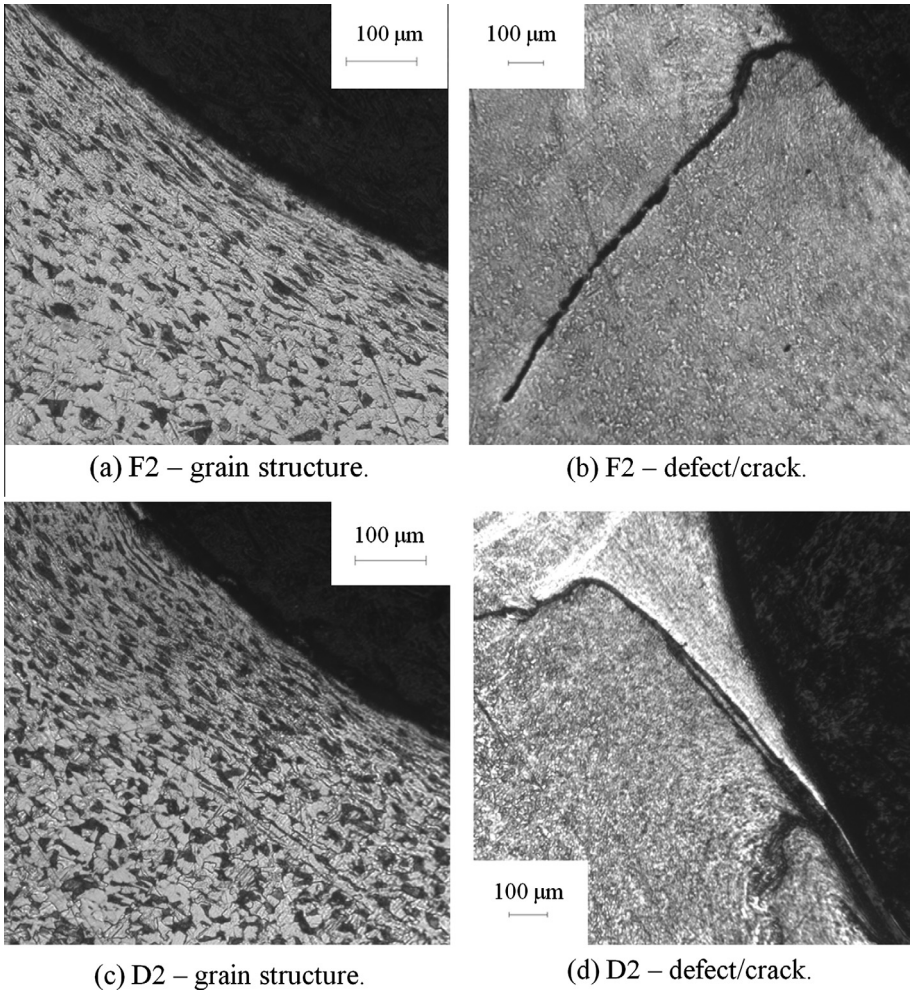


**Fig. 10.** Examples of weld to microstructure and surface defects.

eling. To perform the FE analysis, a 2D plane strain model was chosen and the material properties were assumed to be homogenous and linear elastic. Nominal values of 200,000 MPa and 0.3 were assigned as the elastic modulus ($E$) and Poisson's ratio ($\mu$) respectively. A 1.0 mm node spacing was used in the regions of the specimen far removed from the weld toe. At the weld toe, a much smaller node spacing of 0.02 mm was prescribed. The meshed model of Specimen F1 is shown in Fig. 11(a).

For each specimen type, three weld toe impressions were modeled. Sample SCF distributions are plotted in Fig. 11(b). Peak (surface) SCF values are given for each FE model in Table 5. The mean peak SCF for the as-received welds was 2.99. Proper treatment reduces the peak SCF to 2.09 (robotic, Group E) or 2.12 (manual, Group F). Under-treatment results in a similar or slightly greater reduction in the SCF (2.02 for Group B, 2.03 for Group C), while over-treatment results in a peak SCF that is almost as large as the mean value for the as-received welds (2.82 for Group D).

## 6. Fracture mechanics analysis

While the test results appear to confirm the robustness of UIT and the benefit of treatment and quality control in accordance with the current "best practice"-based guidelines, the small number of samples tested (for the number of variables studied) makes it difficult to draw conclusions regarding the effects of local weld toe property variations on fatigue performance. For this reason, a previously-developed fracture mechanics model was validated and used to investigate these effects.

A full description of the employed strain-based fracture mechanics (SBFMs) model is given in [3]. The basis for the model is the Paris–Erdogan crack growth law, commonly used for linear elastic fracture mechanics (LEFM) analysis, modified to consider crack closure effects and a threshold stress intensity factor (SIF) range, $\Delta K_{th}$, and integrated over a crack depth range, $a_i$ to $a_c$:

$$N = \int_{a_i}^{a_c} \frac{da}{C \cdot \mathrm{MAX}\left(\Delta K_{eff}^{m} - \Delta K_{th}^{m}, 0\right)} \tag{2}$$

where $C$ and $m$ are material constants and $\Delta K_{eff}$ is the effective stress intensity factor range. The main difference between LEFM and SBFM is the calculation of the stress intensity factors (SIFs), $K$. In the latter, the following expression is used [25]:

$$K = Y \cdot E \cdot \varepsilon \cdot \sqrt{\pi \cdot a} \tag{3}$$

where $\varepsilon$ is the local strain at crack depth, $a$, and $Y$ is a correction factor to account for the crack shape, free surface, and the finite thickness of the plate. For the analysis of treated welds, the SBFM model offers considerable advantages over LEFM in terms of its ability to model the evolution of the beneficial compressive residual stresses under VA loading histories.

To calculate the stresses and strains, $\sigma$ and $\varepsilon$, for each load cycle, a Ramberg–Osgood material model is used [26], which requires the cyclic material parameters: $K'$ and $n'$, i.e.:

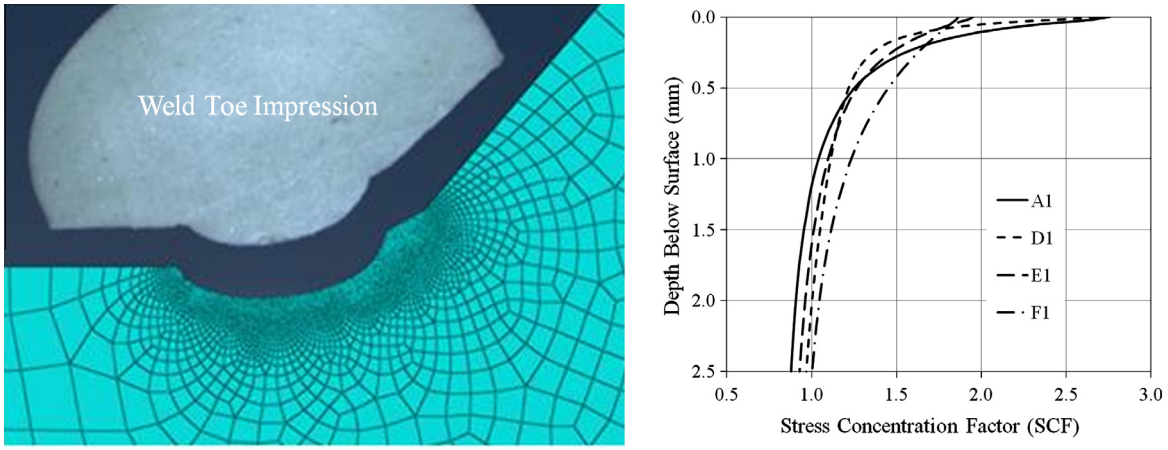


(a) Specimen F1 weld toe impression and FE model. (b) SCF distributions from FE analysis.

**Fig. 11.** FE analysis procedure and SCF distributions.

**Table 5**
Peak stress concentration factors (SCFs).

| Group | As-received | After treatment | | | |
|---|---|---|---|---|---|
| | | Model 1 | Model 2 | Model 3 | $\bar{x}$ |
| A | (A1) 2.76 | – | – | – | – |
| B | (B1) 2.73 | (B1) 2.15 | (B3) 1.96 | (B5) 1.96 | 2.02 |
| C | (C1) 2.37 | (C1) 2.03 | (C3) 1.87 | (C5) 2.20 | 2.03 |
| D | (D1) 2.67 | (D1) 2.68 | (D4) 2.86 | (D6) 3.14 | 2.82 |
| E | (E1) 3.49 | (E1) 1.95 | (E3) 2.06 | (E6) 2.25 | 2.09 |
| F | (F1) 3.89 | (F1) 1.86 | (F4) 2.29 | (F6) 2.21 | 2.12 |

$$\Delta\varepsilon = \frac{\Delta\sigma}{E} + 2 \cdot \left(\frac{\Delta\sigma}{2 \cdot K'}\right)^{1/n'} \quad (4)$$

Strain histories at various depths below the surface are determined using Neuber's rule [26]:

$$\sigma \cdot \varepsilon = \frac{\sigma_{el}^2}{E} \quad (5)$$

where $\sigma_{el}$ is the local elastic stress [3]. Crack closure is modeled using formulas proposed by Newman [27]. These require as input: the maximum stress level, $\sigma_{max}$, the stress ratio, $R$, the flow stress, $\sigma_0$ (i.e. the average of the yield and ultimate strength, $\sigma_y$ and $\sigma_u$), and a plastic constraint factor, $\alpha$.

As discussed in [3], the primary advantage of the employed SBFM model is its ability to predict two crack growth accelerating mechanisms, which can be particularly severe for welds treated with residual stress-based PWTs, namely: (1) compressive underloads can cause relaxation of the compressive residual stresses introduced by the PWT if the total (applied + residual) compressive stress is sufficient to cause a nonlinear material response and (2) large compressive under-loads (or tensile over-loads) can have the effect of reducing the crack opening stress level, and thus increasing the effective portion of the applied stress cycle, for a number of cycles following the extreme loading event.

Table 6 provides values for the input parameters, based on [3], which were assumed to be unaffected by the treatment and were not varied in the sensitivity analysis. Regarding the other input parameters required to implement the SBFM analysis, the following assumptions were made:

- In the initial validation, average SCF distributions for as-received and properly treated welds were assumed, based on the FE results. In the sensitivity analysis, the SCF distribution was varied from the upper bound for the over-treated welds to the lower bound for the properly treated welds.
- In [3], the cyclic material parameters, $K'$ and $n'$ were measured for specimens fabricated out of the same base metal used in the current study. One objective of the current study was to investigate the effects of changes in the local material properties (and in particular the nonlinear material response) due to treatment at the various levels. To do this, the local microhardness measurements were used to estimate $K'$ and $n'$ at each crack depth, using the following relationships from [28]:

$$K' \approx 1.65 \cdot \sigma_u \text{ and } n' \approx 0.15 \quad (6)$$

$$\sigma_u \approx 3.45 \cdot \text{Hardness} \quad (7)$$

In [28], the Brinell hardness number (BHN) is used. However, this is approximately equal to the Vickers hardness (HVN) over the range of interest in the current study. Similarly to the SCF, the initial model validation was performed with average values assumed for as-received and properly treated welds. Linear interpolation was used between measurement points.

- Uniform or multi-linear residual stress distributions were assumed in the analysis, based on a trial-and-error process. For the as-received welds, a uniform distribution with a magnitude of zero was assumed. It is suspected that the actual distribution varies considerably, based on the measurements obtained for the current study and in [3] for the same material and specimen type. However, the overall distribution must be self-equilibrating, and the assumed distribution gives a good prediction of the test results. The distribution assumed for the properly treated weld is shown as a solid line in Fig. 9(b). This distribution also led to close predictions of the test results. It is more-or-less a lower bound of the measured values for properly treated welds, with a distribution shape that agrees well with the measured distributions from other studies, where

**Table 6**
Assumed SBFM input parameters.

| Parameter | Value | Units | Description |
|---|---|---|---|
| $T$ | 9.5 | mm | Nominal plate thickness |
| $C$ | $2.8 \times 10^{-13}$ | N, mm | Paris law constant [3] |
| $m$ | 3.0 | – | Paris law constant |
| $\Delta K_{th}$ | 80.0 | MPa $\sqrt{}$mm | SIF range threshold |
| $\mu$ | 0.002 | – | Crack closure parameter [25] |
| $\sigma_y$ | 396.3 | MPa | Base metal yield strength [3] |
| $\sigma_u$ | 574.3 | MPa | Base metal ultimate strength [3] |
| $E$ | 201.6 | GPa | Elastic modulus [3] |
| $a_c$ | 0.5·T | mm | Critical crack depth |

more measurements were obtained (e.g. [29]). The slope of the distribution was established by fixing the depth at which a uniform tensile distribution is reached at 2.0 mm, and then varying the magnitude of the tensile stress until a self-equilibrating stress distribution was achieved. When this distribution was shifted to represent an average of the measurements for properly treated welds, it tended to over-estimate the test results. One possible explanation for this result it that these compressive residual stresses also vary over a wide range, and so, fatigue failures will be most likely to occur at locations where they are lowest in magnitude. Further investigation would be needed, however, to confirm this. To model the residual stress distributions for under- and over-treated welds, the assumed distribution was shifted as shown by the dashed lines in Fig. 9(b).

– For the validation, an initial defect depth, $a_i$, of 0.15 mm was assumed for as-received and treated welds. An initial crack shape or aspect ratio, $(a/c)_i$, of 0.6 was then fixed and the ratio, $a/c$, was assumed to vary linearly between from 0.6 and to 0.0 at a crack depth of 1.0 mm, based on [3]. This depth and shape were thought to be representative of a weld defect, which would not necessarily be removed by the treatment. Following the model validation, a sensitivity analysis was performed where the defect depth was varied. The goal of this analysis was to study the effect of line defects, such as lack of full removal of the weld toe or surface flaking, resulting from the treatment process itself. For this reason, a constant $a/c$ ratio of zero was assumed in this analysis.

The results of SBFM model validation are shown in Fig. 12. In this Fig. 12, it can be seen that the calculated S–N curves for the as-received welds are very close to the test data. The curve for the CA-UL loading history falls slightly below the data, indicating that the SBFM model, with the values of $K'$ and $n'$ estimated based on the local microhardness, slightly overestimates the negative effect of the under-loads. A similar trend is seen when comparing the model predictions for the properly treated welds. Based on these results, it was determined that the model provided reasonably good predictions of the test data, and could therefore be used to carry out the sensitivity analysis.

In Fig. 13, key results of this analysis are presented. Looking at Figs. 13(a)-(c), the effects of the measured variations in the local microhardness, SCF distribution, and residual stress distribution can be seen and compared with the scatter observed in the test data for the treated welds. In general, it can be seen that the effect of the hardness variations is negligible under CA loading, but much greater for CA-UL loading. When the upper bound of the hardness envelope for the over-treated welds is assumed, the predicted negative effect of under-loads is reduced and appears more in line with the experimental results. Varying the SCF over the investigated range has a larger effect on the S–N curve position. However the upper- and lower-bound curves seem plausible, given the degree of scatter observed in the test data. The greatest effect on the S–N curve position is seen when the residual stresses are varied between the under- and over-treated distributions indicated by the dashed lines in Fig. 9(b). The resulting curves appear to significantly over-predict the degree of scatter observed in the test data. A possible explanation for this result is that there is in fact a high degree of correlation between several of the input parameters. In other words, the high residual stresses measured on the over-treated welds cannot be achieved without also introducing a higher SCF and likely a much higher initial defect depth. Likewise, the

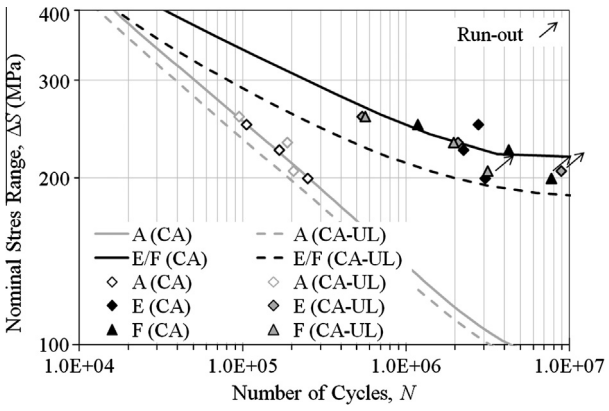


**Fig. 12.** Fracture mechanics analysis results for as-received and properly treated welds.

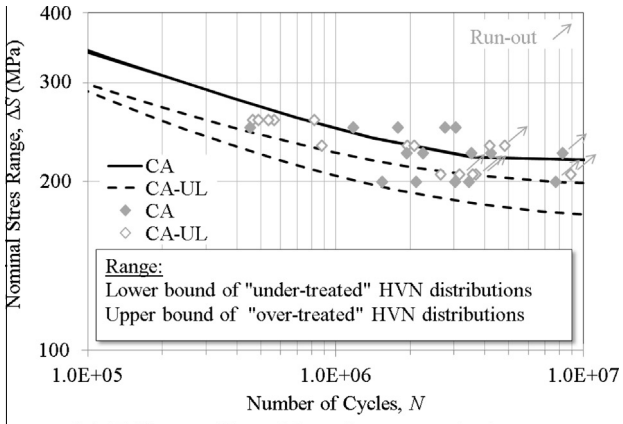


(a) Effect of local hardness variations.

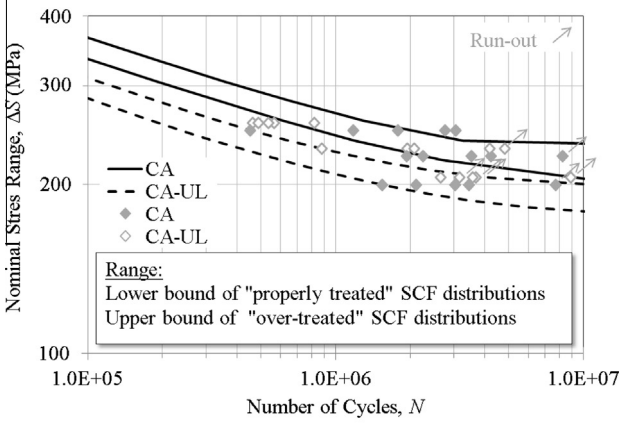


(b) Effect of variations in SCF distribution.

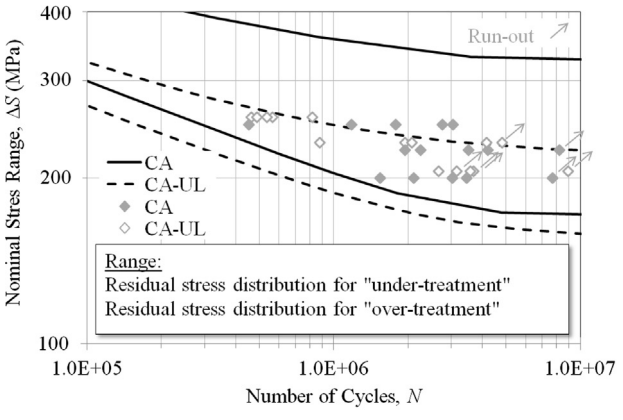


(c) Effect of residual stress variations.

**Fig. 13.** Effect of quality control parameter variations.

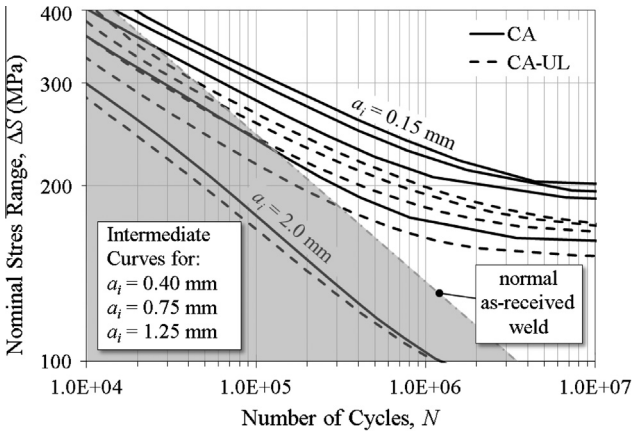


**Fig. 14.** Effect of initial defect depth variations.

SCFs are generally lower for the under-treated welds. It is also possible that the higher residual stresses due to over-treatment have a higher degree of scatter, meaning that the welds will fail at locations where these stresses are lower in magnitude. The noticeably higher degree of scatter in the micro-hardness measurements for the over-treated (Group D) specimens in Fig. 8 would appear to support this hypothesis.

In Fig. 14, the results of the initial defect depth study, for assessing the effects of line defects that may result from the treatment process, are summarized. In this study, analyses were performed for $a_i$ = 0.15, 0.40, 0.75, 1.25, and 2.0 mm. Looking at Fig. 14, it can be seen that the S–N curves shift downwards as the initial defect depth increases. At the highest stress ranges analyzed, the result is that a line defect with a depth as little as 0.4 mm can result in a fatigue life after treatment that is no better than that of a normal as-received weld. At the lower stress ranges, a fatigue life increase due to treatment is still seen, even with the larger defect depths. When the defect depth reaches the depth of the compressive residual stress zone, however, there is a significant drop in the S–N curve, and the fatigue performance of the treated weld is worse than that of a normal as-received weld.

It should be noted that in all of the fracture mechanics analyses, it is assumed that the initial defect will be crack-like and oriented perpendicularly with respect to the loading direction. The large flaking defects observed in the over-treated welds used in the current study (see Fig. 10), tended to be flat and oriented parallel to the loading direction. While presumably somewhat less severe, further study would be needed to predict the effect of this defect geometry analytically.

## 7. Conclusions

Based on the testing and analysis results presented herein, the following conclusions are drawn:

- UIT significantly improved the fatigue lives of the weld specimens tested in the current study, regardless of the treatment level or stress history type. Quality control and treatment in accordance with the current guidelines results in a higher fatigue performance. However, the treatment process is fairly robust in the sense that under- or over-treating within the investigated range of treatment parameter variations still results in a significant fatigue life increase.
- The current recommendations for quality control of welds treated by UIT (e.g. [15]) would have likely been successful in identifying the under- and over-treated weld specimens fabricated for the current study. For identifying over-treatment, indent depth measurements from both the weld and base metal sides, based on weld toe impressions, are recommended as a means of further verifying treatment quality. Evidence of significant flaking as a result of the treatment is another practical means for identifying over-treatment. For identifying under-treatment, indent depth measurements should be used in conjunction with inspection for traces of the original weld toe.
- Through-thickness microhardness and residual stress measurements are not practical for use on actual structures. However, strong correlations were seen between these parameters and the level of treatment quality. On this basis, the use of these methods on sample specimens is recommended for the evaluation or pre-qualification of new UIT methods or procedures.
- The fracture mechanics analysis predicts the fatigue performance of the treated welds and finds it to be most sensitive to variations in the residual stresses and initial defect depth. Microhardness and SCF variations are seen to have less of an effect on fatigue performance.
- The possible negative effects of compressive under-loads on the fatigue performance of the treated welds are conservatively over-predicted by the employed fracture mechanics model.
- An initial defect depth study shows that significant fatigue life increases can still be achieved with a linear defect present as a result of the treatment. However, the treatment benefit decreases with increasing defect depth, and can be completely negated if the defect is sufficiently large.

Further testing, to increase the sample sizes and ranges of the parameter variations would be beneficial, in order to validate the findings of this study and extend their domain of applicability (e.g. to more severe treatment defects, other weld geometries, larger specimens, etc.). On the analytical side, the fracture mechanics study was limited to model validation and deterministic sensitivity analyses. A logical extension of this work would be to perform the analysis probabilistically, so that the effects of variations in the quality control parameters on the design S–N curve can be seen.

## Acknowledgements

The Ministry of Transportation of Ontario (MTO) is gratefully acknowledged for providing financial support for this research. MTO engineers B. Tharmabala, C. Lam, and R. Mihaljevic are thanked for their technical input. Applied Ultrasonics is gratefully acknowledged for providing specimen treatment. S. Abston at Applied Ultrasonics is thanked in particular for his technical input. At the University of Waterloo, technical input and support was provided by Prof. T. Topper, R. Morrison, D. Hirst, and R. Sluban, and assistance in the laboratory was provided by I. Chang and J. Raimbault.

## References

[1] Maddox SJ. Improving the fatigue strength of welded joints by peening. Metal Construct 1985;17:220–4.
[2] Bremen U. Amelioration du comportement à la fatigue d'assemblages soudés: étude et modelisation de l'effet de contraintes residuelles, École Polytechnique Fédérale de Lausanne thesis no. 787, 1989.
[3] Ghahremani K, Walbridge S. Fatigue testing and analysis of peened highway bridge welds under in-service variable amplitude loading conditions. Int J Fatigue 2011;33:300–12.
[4] Haagensen PJ, Maddox SJ. IIW recommendations on post weld fatigue life improvement of steel and aluminium structures. Paris: International Institute of Welding; 2011.
[5] American Welding Society (AWS). Structural welding code: AWS standard D1.1/D1.1M; 2004.
[6] Canadian Standards Association (CSA). Welded steel construction (metal arc welding): CSA standard W59-03; 2003.
[7] Roy S, Fisher JW, Yen BT. Fatigue resistance of welded details enhanced by ultrasonic impact treatment (UIT). Int J Fatigue 2003;25:1239–47.

[8] Roy S. Experimental and analytical evaluation of enhancement in fatigue resistance of welded details subjected to post-weld ultrasonic impact treatment. Doctoral thesis, Department of Civil and Environmental Engineering, Lehigh University; 2006.
[9] American Association of State Highway and Transportation Officials (AASHTO). LFRD bridge design specifications, 4th ed., Washington (DC); 2008.
[10] Kuhlmann U, Durr A, Gunther H-P. Application of post-weld treatment methods to improve the fatigue strength of high strength steels in bridges. IABMAS-06, Porto; 2006.
[11] Huo L, Wang D, Zhang Y. Investigation of the fatigue behaviour of the welded joints treated by TIG dressing and ultrasonic peening under variable-amplitude load. Int J Fatigue 2005;27:95–101.
[12] Marquis G. Failure modes and fatigue strength of improved HSS welds. Eng Fract Mech 2010;77:2051–62.
[13] Yildirim HC, Marquis G. A round robin study of high-frequency mechanical impact (HFMI)-treated welded joints subjected to variable amplitude loading. Weld World 2013;57:437–47.
[14] Ummenhofer T, Weich I, Nitchke-Pagel T. Fatigue life improvement of existing steel bridges. IABMAS-06, Porto; 2006.
[15] American Association of State Highway and Transportation Officials (AASHTO). LRFD bridge construction specifications: interim revisions. Washington (DC); 2008.
[16] Yildirim HC, Marquis G. Fatigue strength improvement factors for high strength steel welded joints treated by high frequency mechanical impact. Int J Fatigue 2012;44:168–76.
[17] Yildirim HC, Marquis G, Barsoum Z. Fatigue assessment of high frequency mechanical impact (HFMI)-improved fillet welds by local approaches. Int J Fatigue 2013;52:57–67.
[18] Canadian Institute of Steel Construction (CISC). Handbook of steel construction, 9th ed., Toronto; 2006.
[19] Tehrani Yekta R. Acceptance criteria for ultrasonic impact treatment (UIT). M.A.Sc. Thesis, University of Waterloo; 2012.
[20] Lugg MC. TSC inspection systems; 2008.
[21] Canadian Standards Association (CSA). Canadian highway bridge design code: CAN/CSA-S6-06, 2006.
[22] Hobbacher A. Recommendations for fatigue design of welded joints and components. International Institute of Welding: Doc. XIII-1965-03/XV-1127-03; 2005.
[23] American Society for Testing and Materials (ASTM). Standard test method for knoop and vickers hardness of materials: ASTM E384-11; 2011.
[24] Weich I, Ummenhofer T, Nitschke-Pagel T, Dilger K, Eslami H. Fatigue behaviour of welded high-strength steels after high frequency mechanical post-weld treatments. Weld World 2009;53:R322–32.
[25] Khalil M, Topper TH. Prediction of crack-opening stress levels for 1045 as-received steel under service loading spectra. Int J Fatigue 2003;25(2):149–57.
[26] Dowling NE. Mechanical behaviour of materials. Upper Saddle River, New Jersey: Pearson Education Inc.; 2007.
[27] Newman JC. A crack opening stress equation for fatigue crack growth. Int J Fract 1994;24:R131–5.
[28] Baumel A, Seeger T. Materials data for cyclic loading – supplement 1. New York: Elsevier Science Publishing Company; 1990.
[29] Cheng X, Fisher JW, Prask HJ, Gnäupel-Herold T, Yen BT, Roy S. Residual stress modification by post-weld treatment and its beneficial effect on fatigue strength of welded structures. Int J Fatigue 2003;25:1259–69.